Available online at http://scik.org
Commun. Math. Biol. Neurosci. 2020, 2020:70
https://doi.org/10.28919/cmbn/4947
ISSN: 2052-2541

NEW AUTOMATED OPTIMAL VACCINATION CONTROL WITH A MULTI-REGION SIRS EPIDEMIC MODE

BOUTAYEB HAMZA, BIDAH SARA, ZAKARY OMAR*, AGMOUR IMANE, RACHIK MOSTAFA

Laboratory of Analysis, modeling and simulation, Department of mathematics and computer sciences, Faculty of sciences Ben M'Sik, University Hassan II of Casablanca, Morocco

Abstract. Many mathematical models describing the evolution of infectious diseases underestimate the effect of the Spatio-temporal spread of epidemics. Currently, the COVID-19 epidemic shows the importance of taking into account the spatial dynamic of epidemics and pandemics. In this paper, we consider a multi-region discrete-time SIRS epidemic model that describes the spatial spread of an epidemic within different geographical zones assumed to be connected with the movements of their populations (cities, towns, neighbors...).

Judging by the fact that there are several restrictions in medical resources and some delay in decision-making, the authorities and health decision-makers must define a threshold of infections in order to determine if a zone is epidemic or not yet. We propose a new approach of optimal control by defining new importance functions to identify affected zones and then the need for the control intervention. This optimal control strategy allows to reduce the infectious individuals and increase the number of recovered ones in the targeted domain and this with an optimal cost. Numerical results are provided to illustrate our findings by applying this new approach in the Casablanca-Settat region of Morocco. We investigate different scenarios to show the most effective scenario, based on thresholds' values.

Keywords: optimal control; multi-region; SIRS; vaccination; epidemic model.

2010 AMS Subject Classification: 39A05, 39A45, 39A60, 93C35, 93C55.

*Corresponding author

E-mail address: zakaryma@gmail.com

Received August 14, 2020

1. INTRODUCTION

A quarter to a third of all deaths in the world are due to infectious diseases, as reported by the World Health Organization (WHO). It also noted that infectious diseases made up four to five of the ten leading causes of death in 2008 [1].

In the fields of mathematical biology [2] and mathematical epidemiology (ME) [3], it is found that mathematical models have been an important tool in the analysis of the epidemiological characteristics of infectious diseases since the pioneering work of Kermack and McKendrick [1], I.e. the construction and analysis of mathematical models describing the spread and control of infectious diseases, epidemics and pandemics, which have a considerable influence. National and international health agencies often use mathematical models of epidemics in the evaluation of public health policies. Recently, an important number of articles in ME sector are published by high-profile research medical journals [4, 5, 6, 7, 8]. The evolution analysis of the epidemics from their population systems [9] and in different geographical areas [10, 11, 12] has become feasible thanks to epidemiological modeling. That allowed these last to undergo a big evolution over the past decades.

One of the main assumption in many mathematical models of epidemics is that the population can be divided into an ensemble of separate states. These states are defined according to the state of the disease. The simplest model, which calculates the theoretical number of people infected with a contagious disease in a closed population over time, described by Kermack and Mckendrick (1927), consists of three components: susceptible (S), infected (I) and recovered (R). The disease states are defined as follows:

• Susceptible: Individuals that have never been infected and can thus contract the disease. Once infected, they move to the infected state.

• Infected: Individuals that can transmit the disease to susceptible individuals. The time that individuals spend in the infected state is the infectious period; then they enter the recovered state.

• Recovered: Individuals in recovery are assumed to be immune for life [13].

Susceptible-Infected-Susceptible (SIS) epidemic models have been applied to situations in which it is supposed that an infected population could move immediately to the susceptible

compartment after being recovered from an infection due to the lack of immunization. This kind of compartmental models is also useful to model the evolution of many phenomena in different situations, see as examples, subjects treated in [14, 15]

Susceptible-Infected-Removed-Susceptible (SIRS) epidemic models have been applied to situations in which it has been supposed that a removed population could move to the susceptible compartment after being healed from an infection due to the loss of its immunity. This kind of compartmental models is very useful to model the evolution of many phenomena, see as examples, subjects treated in [16, 17, 18].

Different from the SIR model, the SIRS model also considers ”short-term immunity”. The so-called ”short-term immunity” is that the immune individual becomes susceptible individual after a while. [19]

Mathematical models have become important tools in analyzing the spread and control of infectious diseases. The model formulation process clarifies assumptions, variables and parameters. There have been many studies that have mathematically analyzed infectious diseases and several optimization approaches have been proposed to prove their effectiveness in the control of certain diseases, mainly, HIV, Ebola [11, 20, 21, 22, 23], ZIKA Virus [24], Malaria [25, 26], Influenza Pandemic [9, 27], Cancer [28, 29], Tuberculosis [30, 31], COVID-19 [32] and even in other areas of research [33, 34, 35, 36, 37].

In the history of all these diseases, we can notice their spread from one region to another, and recently the COVID-19 pandemic from its epicenter of Wuhan in China has spread to all parts of the world, which makes taking into account the spatial spread of diseases more important during modeling processes.

The authors in [10] present the first work in the modeling and control of spatio-temporal spread of an epidemic using a multi-region SIR discrete-time model, as a generalization of the concept of classical models and aiming at a description of the evolution of pandemics, Zakary et al proposed a new approach of modeling of the spread of epidemics from one area to another using finite-dimensional models for the Spatio-temporal propagation of epidemics as an alternative of the partial derivatives models which are of infinite dimension. The authors also suggested some control strategies such as awareness-raising, vaccination, and travel-restriction

approaches that could prevent specific infectious diseases such as HIV / AIDS, Ebola, or other epidemics in general [10, 12, 20, 11, 14], other researchers have shown the power and effectiveness of educational workshops and awareness programs in reducing the number of infected individuals [38, 39, 21].

In this paper, we propose a new optimal control approach mainly based on a multi-regions discrete-time system and a new form of multi-objective optimization criteria with importance indices and which is subject to multi-points boundary value optimal control problems. With more clarifications and essential details, we devise here a multi-regions discrete model for the study of the spread of an epidemic in M different regions, and analyze the effectiveness of vaccination (or awareness) optimal control strategies when vaccination (or awareness) campaigns are organized in infected zones. Here, we study the case when controls are applied to people who belong to all those regions and which are supposed to be reachable for every agent (nurse, doctor or media) who is responsible for the accomplishment of control strategies followed against the disease.

We consider an area as an infected zone if its number of infected individuals exceeds a threshold defined by the health decision-makers. Therefore, by varying the values of this threshold and then simulating the infection situation for different values of these thresholds shows that it is necessary to think about reducing the time between the first infection and the implementation of the control strategy. Unexpected results that in some situations the neighboring regions infected and its number of infections exceeds the threshold before the number of infections of the region source. This makes the implementation of the control strategies in the neighboring zones more important.

In our modeling approach we divided the studied area Ω into different zones that we call cells. A cell $C_j \in \Omega$ can represent a city, a country or a larger domain. These cells are supposed to be connected by movements of their populations within the domain Ω. We define also a neighboring cells C_k of the cell C_j all zones connected with C_j via every transport mean, thus a cell $C_j \in \Omega$ can have more than one neighboring cell. Here, we suppose that a cell can be infected due to movements of infected people which enter only from its neighboring zones.

We carry out the map of the studied area and then we use different threshold values in the controlled multi-region SIRS model to simulate the epidemic spread within the Casablanca-Settat region illustrated in the Fig.1, by combining the ArcGIS and Matlab programs.

The paper is organized as follows: Section 2. presents the discrete-time multi-region SIRS epidemic system. In Section 3., we announce theorems of the existence and characterization of the sought optimal controls functions related to the optimal control approach we propose. Finally, in section 4., we provide simulations of the numerical results applied to the Casablanca-Settat region as domain of interest.

FIGURE 1. The geographical studied zone Ω: (a) Discretization on two regions Casablanca-Settat . (b) Discretization of the whole studied zone on provinces with names.

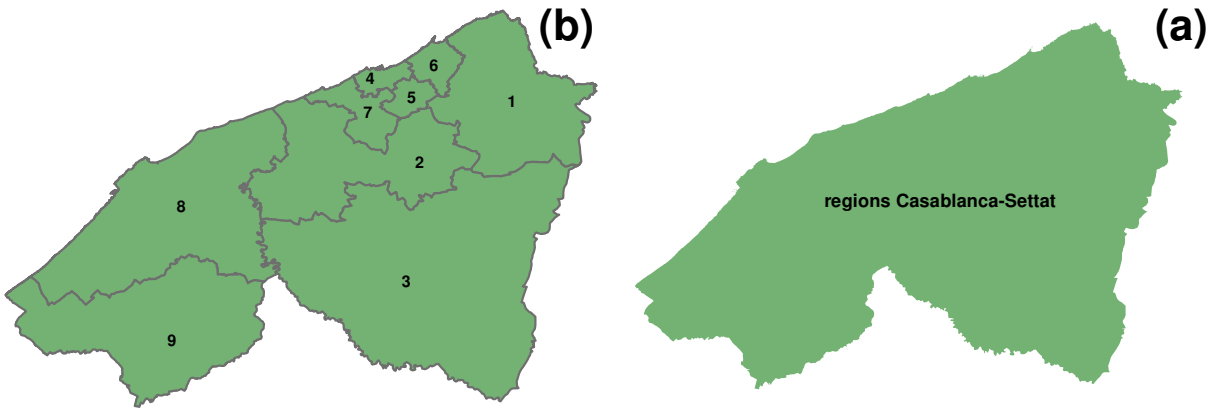

2. MODEL DESCRIPTION AND DEFINITIONS

Based on same modeling assumptions of Reference [10], we assume that there are M geographical regions denoted C_j (sub-domains) of the domain studied Ω

$$\Omega = \bigcup_{j=1}^{M} C_j$$

where C_j can represent a city, a country or a larger domain. We note by $V(C_j)$, the vicinity set, composed by all neighboring cells of C_j given by

$$V(C_j) = \left\{C_k \in \Omega \ / \ C_j \cap C_k \neq \emptyset\right\}$$

where $C_j \cap C_k \neq \emptyset$ means that there exists at least one mean of transport between C_j and C_k. Note that this definition of $V(C_j)$ is more general where it defines a more general form of vicinity regardless the geographical location of zones.

For example, in the Table 1 we can see that the studied area consists of 9 zones.

The multi-regional discrete-time SIR model associated to C_j with $\varepsilon_i^{C_j} = 0$ (no control is introduced yet in C_j) is then

$$S_{i+1}^{C_j} = S_i^{C_j} - \sum_{C_k \in V(C_j)} \beta^{C_j^k} \frac{I_i^{C_k}}{N_i^{C_j}} S_i^{C_j} + \left(N_i^{C_j} - S_i^{C_j}\right) d_j + \theta_j R_i^{C_j} \tag{1}$$

$$I_{i+1}^{C_j} = I_i^{C_j} + \sum_{C_k \in V(C_j)} \beta^{C_j^k} \frac{I_i^{C_k}}{N_i^{C_j}} S_i^{C_j} - \gamma_j I_i^{C_j} - d_j I_i^{C_j} - \alpha^{C_j} I_i^{C_j} \tag{2}$$

$$R_{i+1}^{C_j} = R_i^{C_j} + \gamma_j I_i^{C_j} - d_j R_i^{C_j} - \theta_j R_i^{C_j} \tag{3}$$

where the disease transmission coefficient $\beta^{C_j^k} > 0$ is the proportion of adequate contacts in domain C_j between a susceptible from C_j $(j = 1, ..., M)$ and an infective from another domain C_k, d_j is the birth and death rate and γ_j is the recovery rate ans α^{C_j} is the proportion of mortality due to the disease. The biological background requires that all parameters be non-negative. θ_j is the proportion that a recovered becomes again a susceptible. $S_i^{C_j}$, $I_i^{C_j}$ and $R_i^{C_j}$ are the numbers of individuals in the susceptible, infective, and removed compartments of C_j at time i, respectively, and $N_i^{C_j} = S_i^{C_j} + I_i^{C_j} + R_i^{C_j}$ is the population size corresponding to domain C_j at time i. It is clear that the population size is not constant for all $i \geq 0$.

Nb	Zone	Population	Nb	Zone	Population	Nb	Zone	Population
1	BEN SLIMANE	233123	4	Casablanca	3359818	7	Nouaceur	333604
2	Berrechid	484518	5	Mediouna	172680	8	El Jadida	786716
3	Settat	634184	6	Mohammadia	404648	9	Sidi Bennour	452448

TABLE 1. Populations of the regions: Casablanca-Settat

3. The Model With Vaccination

3.1. Presentation of the model with the control. In this section, we introduce a control variable $u_i^{C_j}$ that characterizes the effectiveness of the vaccination in the above mentioned model (1-3). This control in some situations can represent the effect of the awareness and media programs [11, 20].

In almost all infectious diseases, the authorities determine the threshold of risk based on many factors, such as availability of medical equipment, budgets, and medical personnel ... Thus, they can wait some time to see the course of events before the intervention. If the number of casualties exceeds this limit, decision-makers have no choice but to start trying to control the situation. This motivate us to define a Boolean function $\varepsilon_i^{C_j} = f^{C_j}(I)$ ($\varepsilon_i^{C_j} = 1$ or $\varepsilon_i^{C_j} = 0$) associated to domain C_j, that will be called the importance function of C_j. Where $\varepsilon_i^{C_j}$ is either equaling to 1, in the case when the number of infected of the cell C_j at instant i is greater than or equal to the threshold $\mathscr{I}^{C_j}$ defined by the authorities and health decision-makers, or $\varepsilon_i^{C_j} = 0$ otherwise. Therefore, we define the importance function $\varepsilon_i^{C_j}$ by the Heaviside step function H as follows

$$\varepsilon_i^{C_j} = H\left(I_i^{C_j} - \mathscr{I}^{C_j}\right) = \begin{cases} 0 & I_i^{C_j} < \mathscr{I}^{C_j} \\ 1 & I_i^{C_j} \geq \mathscr{I}^{C_j} \end{cases}$$

Then for a given domain $C_j \in \Omega$, the model is given by the following equations

$$\begin{aligned} S_{i+1}^{C_j} &= S_i^{C_j} - \sum_{C_k \in V(C_j)} \beta^{C_j^k} \frac{I_i^{C_k}}{N_i^{C_j}} S_i^{C_j} + \left(N_i^{C_j} - S_i^{C_j}\right) d_j + \theta_j R_i^{C_j} \\ &\quad - \varepsilon_i^{C_j} u_i^{C_j} S_i^{C_j} \end{aligned} \tag{4}$$

$$I_{i+1}^{C_j} = I_i^{C_j} + \sum_{C_k \in V(C_j)} \beta^{C_j^k} \frac{I_i^{C_k}}{N_i^{C_j}} S_i^{C_j} - \gamma_j I_i^{C_j} - j I_i^{C_j} - \alpha^{C_j} I_i^{C_j} \tag{5}$$

$$R_{i+1}^{C_j} = R_i^{C_j} + \gamma_j I_i^{C_j} - d_j R_i^{C_j} - \theta_j R_i^{C_j} + \varepsilon_i^{C_j} u_i^{C_j} S_i^{C_j} \tag{6}$$

Our goal is obviously to try to minimize the population of the susceptible group and the cost of vaccination in all affected regions. Our control functions taking values between $u_{min}^{C_j}$ and $u_{max}^{C_j}$, where $u_{min}^{C_j}, u_{max}^{C_j} \in]0,1[$, $\forall C_j \in \Omega$.

3.2. An optimal control approach. We devise in this paper an optimal control approach for each region with different importance functions $\varepsilon_i^{C_j}$, $j = 1, ..., M$. We characterize an optimal control that minimize the number of the infected people and maximize the ones in the removed category for all affected regions. Then, we are interested by minimizing the functional

$$J(u) = \sum_{k=1}^{M} \varepsilon_i^{C_k} J^{C_k}(u^{C_k}) \tag{7}$$

where $J^{C_k}(u^{C_k})$ is given by

$$\begin{aligned} J^{C_j}(u^{C_j}) &= \left(\alpha_I^{C_j} I_N^{C_j} - \alpha_R^{C_j} R_N^{C_j}\right) \\ &+ \sum_{i=0}^{N-1} \left(\alpha_I^{C_j} I_i^{C_j} - \alpha_R^{C_j} R_i^{C_j} + \frac{A^{C_j}}{2}(u_i^{C_j})^2\right) \end{aligned} \tag{8}$$

where $A^{C_j} > 0$, $\alpha_I^{C_j} > 0$, $\alpha_R^{C_j} > 0$ are the weight constants of control, the infected and the removed in region C_j respectively, and $u = \left(u^{C_1}, ..., u^{C_M}\right)$ where $u^{C_j} = \left(u_0^{C_j}, ..., u_{N-1}^{C_j}\right)$.
Here, our goal is to minimize the number of infected people, minimize the systemic costs attempting to increase the number of removed people in each C_j (with $\varepsilon_i^{C_j} = 1$). In other words, we are seeking an optimal control u^* such that

$$J(u^*) = min\{J(u)/u \in U\}$$

where U is the control set defined by

$$U = \{u = \left(u^{C_1}, ..., u^{C_M}\right)/u^{C_j} \in U^{C_j}, \forall C_j \in \Omega\}$$

with

$$U^{C_j} = \{u^{C_j} \text{ measurable}/u_{min}^{C_j} \leq u_i^{C_j} \leq u_{max}^{C_j}, i = 0, ..., N-1\}$$

where $u_{min}^{C_j} \in]0,1[$ and $u_{max}^{C_j} \in]0,1[, \forall C_j \in \Omega$. The sufficient condition for existence of an optimal control for the problem follows from theorem 1 . At the same time, by using Pontryagin's Maximum Principle [42] we derive necessary conditions for our optimal control in theorem 2. For this purpose, we define the Hamiltonian as

$$
\begin{aligned}
\mathscr{H} &= \sum_{j=1}^{M} \varepsilon_i^{C_j}\left(\alpha_I^{C_j} I_i^{C_j} - \alpha_R^{C_j} R_i^{C_j} + \frac{A^{C_j}}{2}(u_i^{C_j})^2\right) \\
&+ \sum_{j=1}^{M} \varepsilon_i^{C_j}\left[\zeta_{1,i+1}^{C_j}\left[S_i^{C_j} - \sum_{C_k \in V(C_j)} \beta^{C_j^k} \frac{I_i^{C_k}}{N_i^{C_j}} S_i^{C_j}\right.\right. \\
&\quad \left. + \left(N_i^{C_j} - S_i^{C_j}\right) d_j - \varepsilon_i^{C_j} u_i^{C_j} S_i^{C_j} + \theta_j R_i^{C_j}\right] \\
&+ \zeta_{2,i+1}^{C_j}\left[I_i^{C_j} + \sum_{C_k \in V(C_j)} \beta^{C_j^k} \frac{I_i^{C_k}}{N_i^{C_j}} S_i^{C_j}\right. \\
&\quad \left. - \gamma_j I_i^{C_j} - d_j I_i^{C_j} - \alpha^{C_j} I_i^{C_j}\right] \\
&+ \zeta_{3,i+1}^{C_j}\left[R_i^{C_j} + \gamma_j I_i^{C_j} - d_j R_i^{C_j} - \theta_j R_i^{C_j} + \varepsilon_i^{C_j} u_i^{C_j} S_i^{C_j}\right]\Big] \qquad (9)
\end{aligned}
$$

Theorem 1. *(Sufficient conditions) For the optimal control problem given by (7) along with the state equations (4-6), there exists a control $u^* \in U$ such that*

$$J(u^*) = min\{J(u)/u \in U\}$$

Proof. See Dabbs, K [[40], Theorem 1]. □

Theorem 2. *(Necessary Conditions)*

Given the optimal control u^* and solutions S^{C_j*}, I^{C_j*} and R^{C_j*}, there exists $\zeta_{k,i}^{C_j}$, $i = 1...N$, $k = 1,2,3$, the adjoint variables satisfying the following equations

$$
\begin{aligned}
\Delta\zeta_{1,i}^{C_j} &= -\varepsilon_i^{C_j}\left[\left(1 - \sum_{C_k \in V(C_j)} \beta^{C_j^k} \frac{I_i^{C_k}}{N_i^{C_j}} - d_j - \varepsilon_i^{C_j} u_i^{C_j}\right)\zeta_{1,i+1}^{C_j}\right. \\
&\quad \left. + \sum_{C_k \in V(C_j)} \beta^{C_j^k} \frac{I_i^{C_k}}{N_i^{C_j}} \zeta_{2,i+1}^{C_j} + \varepsilon_i^{C_j} u_i^{C_j} \zeta_{3,i+1}^{C_j}\right] \qquad (10) \\
\Delta\zeta_{2,i}^{C_j} &= -\varepsilon_i^{C_j}\left[\alpha_I^{C_j} - \beta^{C_j^j} \frac{S_i^{C_j}}{N_i^{C_j}} \zeta_{1,i+1}^{C_j}\right. \\
&\quad \left. + \left(1 + \beta^{C_j^j} \frac{S_i^{C_j}}{N_i^{C_j}} - \gamma_j - d_j - \alpha^{C_j}\right)\zeta_{2,i+1}^{C_j} + \gamma_j \zeta_{3,i+1}^{C_j}\right] \qquad (11) \\
\Delta\zeta_{3,i}^{C_j} &= -\varepsilon_i^{C_j}\left[-\alpha_R^{C_j} + (1 - d_j - \theta_j)\zeta_{3,i+1}^{C_j} + \zeta_{1,i+1}^{C_j}\theta_j\right] \qquad (12)
\end{aligned}
$$

where $\zeta_{1,N}^{C_j}=0, \zeta_{2,N}^{C_j}=\varepsilon_i^{C_j}\alpha_I^{C_j}, \zeta_{3,N}^{C_j}=-\varepsilon_i^{C_j}\alpha_R^{C_j}$ *are the transversality conditions. In addition,*

$$u^*=\left(u^{C_1*},...,u^{C_M*}\right)$$

where $u^{C_j}=\left(u_0^{C_j},...,u_{N-1}^{C_j}\right)$*, is given by*

$$u_i^{C_j*}=min\left\{max\left\{u_{min}^{C_j},\frac{\left(\zeta_{1,i+1}^{C_j}-\zeta_{3,i+1}^{C_j}\right)S_i^{C_j}}{A^{C_{pq}}}\right\},u_{max}^{C_j}\right\},\ if\ \varepsilon_i^{C_j}=1 \tag{13}$$

$$u_i^{C_j*}=0,\ otherwise \tag{14}$$

Proof. Using Pontryagin's Maximum Principle [41] and for $j\in I_C$, we obtain the following adjoint equations

$$\begin{aligned}
\Delta\zeta_{1,i}^{C_j} &= -\frac{\partial\mathscr{H}}{\partial S_i^{C_j}}= -\varepsilon_i^{C_j}\left[\left(1-\sum_{C_k\in V(C_j)}\beta^{C_j^k}\frac{I_i^{C_k}}{N_i^{C_j}}-d_j-\varepsilon_i^{C_j}u_i^{C_j}\right)\zeta_{1,i+1}^{C_j}\right.\\
&\quad\left.+\left(\sum_{C_k\in V(C_j)}\beta^{C_j^k}\frac{I_i^{C_k}}{N_i^{C_j}}\zeta_{2,i+1}^{C_j}+\varepsilon_i^{C_j}u_i^{C_j}\zeta_{3,i+1}^{C_j}\right)\right]\\
\Delta\zeta_{2,i}^{C_j} &= -\frac{\partial\mathscr{H}}{\partial I_i^{C_j}}= -\varepsilon_i^{C_j}\left[\alpha-\beta^{C_j^j}\frac{S_i^{C_j}}{N_i^{C_j}}\zeta_{1,i+1}^{C_j}\right.\\
&\quad\left.+\left(1+\beta^{C_j^j}\frac{S_i^{C_j}}{N_i^{C_j}}-\gamma_j-d_j-\alpha^{C_j}\right)\zeta_{2,i+1}^{C_j}+\gamma_{pq}\zeta_{3,i+1}^{C_j}\right]\\
\Delta\zeta_{3,i}^{C_j} &= -\frac{\partial\mathscr{H}}{\partial R_i^{C_j}}= -\varepsilon_i^{C_j}\left[-\alpha_R^{C_j}+(1-d_j-\theta_j)\,\zeta_{3,i+1}^{C_j}+\zeta_{1,i+1}^{C_j}\theta_j\right]
\end{aligned}$$

with $\zeta_{1,N}^{C_j}=0, \zeta_{2,N}^{C_j}=\varepsilon_i^{C_j}\alpha_I^{C_j}, \zeta_{3,N}^{C_j}=-\varepsilon_i^{C_j}\alpha_R^{C_j}$. To obtain the optimality conditions we take the variation with respect to control $u_i^{C_{pq}}$ and set it equal to zero and $\varepsilon_i^{C_j}=1$:

$$\frac{\partial\mathscr{H}}{\partial u_i^{C_j}}=A^{C_j}u_i^{C_j}-\zeta_{1,i+1}^{C_j}S_i^{C_j}+\zeta_{3,i+1}^{C_j}S_i^{C_j}=0$$

Then, we obtain the optimal control

$$u_i^{C_j}=\frac{\left(\zeta_{1,i+1}^{C_j}-\zeta_{3,i+1}^{C_j}\right)S_i^{C_j}}{A^{C_j}}$$

And

$$u_i^{C_j}=0,\text{ if }\varepsilon_i^{C_j}=0$$

By the bounds in U (and U^{C_j}) of the control, it is easy to obtain $u_i^{C_j*}$ in the following form

$$u_i^{C_j*} = min\left\{ max\left\{ u_{min}^{C_j}, \frac{\left(\zeta_{1,i+1}^{C_j} - \zeta_{3,i+1}^{C_j}\right) S_i^{C_j}}{A^{C_{pq}}} \right\}, u_{max}^{C_j} \right\}, \text{ if } \varepsilon_i^{C_j} = 1$$

$$u_i^{C_j*} = 0, \text{otherwise}$$

□

4. NUMERICAL RESULTS.

Parameter	Description	Value
β	Infection rate	1×10^{-3}
d	Birth and death rate	1×10^{-5}
γ	Recovery rate	1×10^{-5}
α	Death due to the infection	1×10^{-4}
θ	loss of immunity	1×10^{-6}

TABLE 2. Parameters values of β, d, θ, α and γ utilized for the resolution of all multi-regions discrete systems and then leading to simulations obtained from Fig.2 to Fig.19, with the initial populations given in Table 1.

In this section, we present numerical simulations associated to the above mentioned optimal control problem. We write a code in $MATLAB^{TM}$ and simulated our results for several scenarios. The optimality systems is solved based on an iterative discrete scheme that converges following an appropriate test similar the one related to the Forward-Backward Sweep Method (FBSM). The state system with an initial guess is solved forward in time and then the adjoint system is solved backward in time because of the transversality conditions. Afterwards, we update the optimal control values using the values of state and co-state variables obtained at the previous steps. Finally, we execute the previous steps till a tolerance criterion is reached.

4.1. Area of interest. We chose the Casablanca-Settat region as the studied area Ω in this paper because we are convinced that we can find some useful data to support our work. They are the most populated and dynamic regions of Morocco, which contain They contain also the

Casablanca city as the economic and industrial capital of Morocco because with its demographic growth and continuous development of the industrial sector, and the 14 other provinces (see Fig.1), in order to illustrate the objective of our work.

Fig.1 illustrates an example of discrete geographical zones of Casablanca-Settat regions (Morocco) where $M = 9$, this image was originally made based on information from [43].

4.2. Geographical vicinity. A shape-file is a simple, non topological format for storing the geometric location and attribute information of geographic features. Geographic features in a shape-file can be represented by points, lines, or polygons (areas). The workspace containing shape-files may also contain database tables, which can store additional attributes that can be joined to a shape-file's features [44]. ArcMap is a central application used in ArcGIS software, where we can view and explore GIS database for our study area, and where we assign symbols and create map layouts for printing or publication. In this application we can represent geographic information as a set of layers and other elements in a map. Common map elements of a map include the data frame containing the map layers for a given extent [45]. Neighborhood tools create output values for each cell location based on the location value and the values identified in a specified neighborhood [46]. We use this tool to create the neighborhood $V(C_j)$ of each separated zone C_j within the area of interest Ω. For instance

$$V(C_4) = \{C_5, C_6, C_7\}$$

Without loss of generality, we set the same infection threshold for all zones, therefore, hereafter we noteI^{C_j}as I_{min}.

4.3. Scenario 0: Simulation of the multi-region model without any control. In all the rest geographical figures, we consider four time steps (a) $i = 0$, (b) $i = 40$, (c) $i = 80$, and (d) $i = 120$, (e) $i = 160$ and (f) $i = 200$. Dark color represents the highest values. Geographical figures show the transmission of infection between different zones while associated graphs show states' changes over time.

*

FIGURE 2. Susceptibl without any control

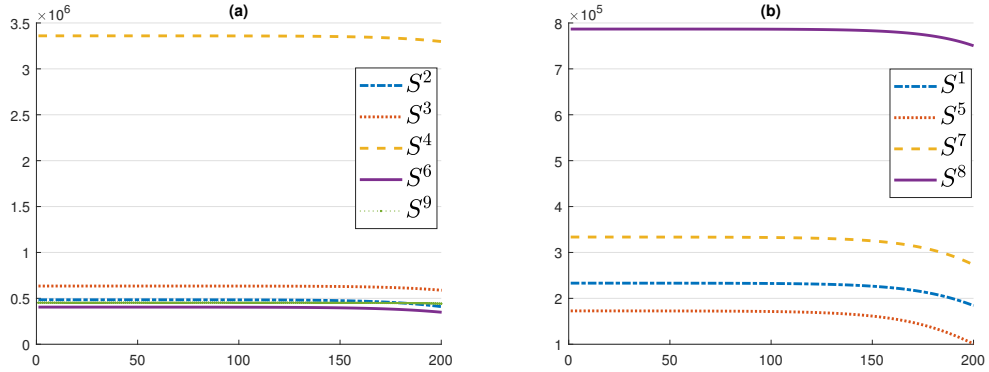

FIGURE 3. Susceptible without any control

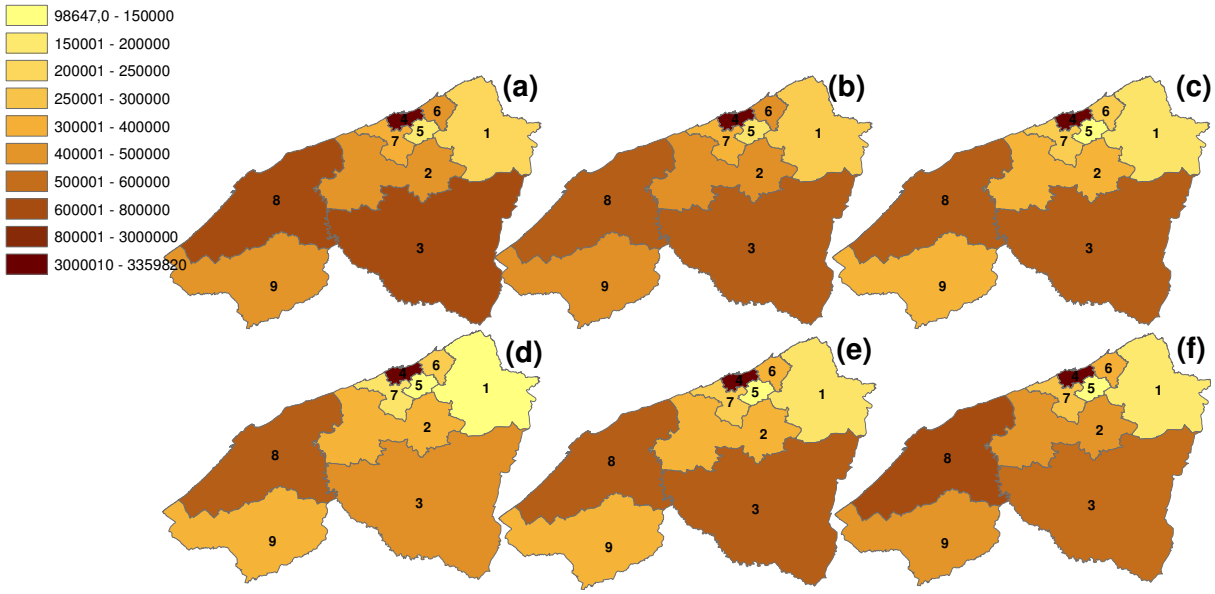

Fig.3(a), (b), (c),(d),(e) and (f) indicate the geographical distribution of susceptible people in the 9 regions without any control strategy at the moments $i = 0$, $i = 40$, $i = 80$, $i = 120$, $i = 160$ and $i = 200$ respectively.

While we see in Fig.2 and 3 represent the evolution of the susceptible individual without controls in the different regions.

We see from Fig.2 and 3 that the number of susceptible people from all regions except C_9 are constant until the instant $i = 150$ then decreases betwin 3.8 10^3 and 7.7 10^4 person at the end. In regions C_2, C_3 and C10 the number of susceptible people is almost constant the number of susceptible C_9 is constant until $i = 160$ and decreases about 10^4.

FIGURE 4. infected without any control

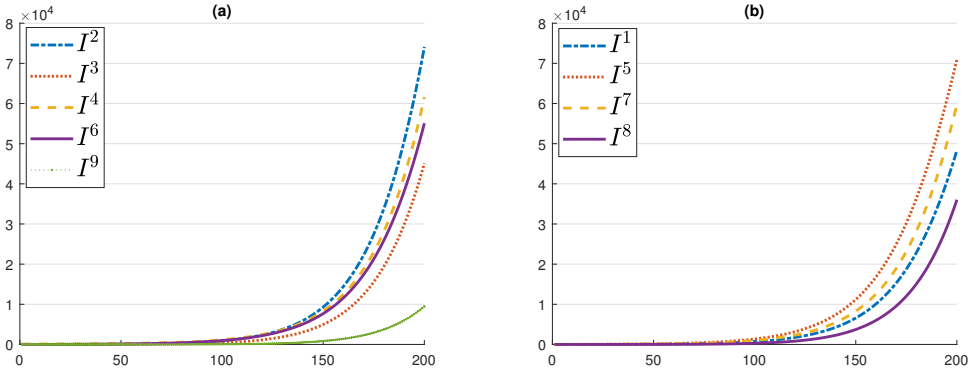

FIGURE 5. Infected without any control

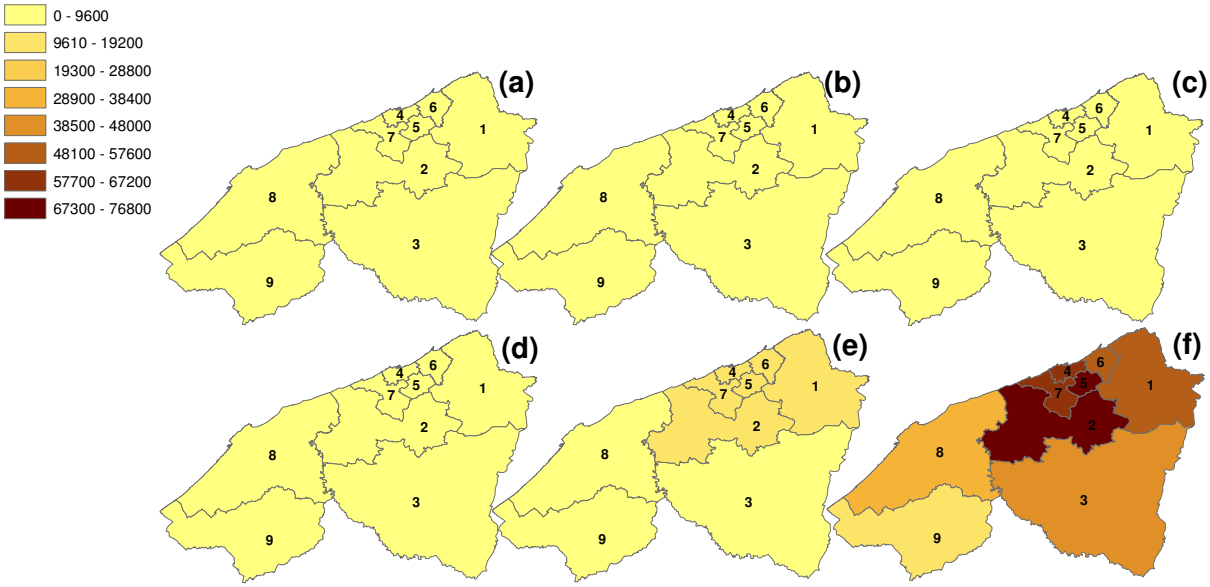

Fig.4 and Fig.5 represent the evolution of the infected without controls in the different regions. In the Fig.4, we note that at the beginning, all the regions did not record any infection until moment $i = 120$ and from the moment $i = 120$, the number of infected increases exponentially, and we see it clearly in the Fig.5 which has kept the same display in the four first maps (Fig.5 (a), (b), (c) and (d)) which means that the number of infected did not exceed 9600 in all regions. In the instant $i = 160$, the region of Casablanca (C_4) and the neighboring regions C_1, C_2, C_5, C_6, C_7 exceeded the 9600 infected. The final state $i = 200$ has seen strong evolution, all the regions have exceeded 19200 infected except C_9 which has just reached 10^5, regions C_2 and C_5 have exceeded 67300 infected.

FIGURE 6. Romoved without any control

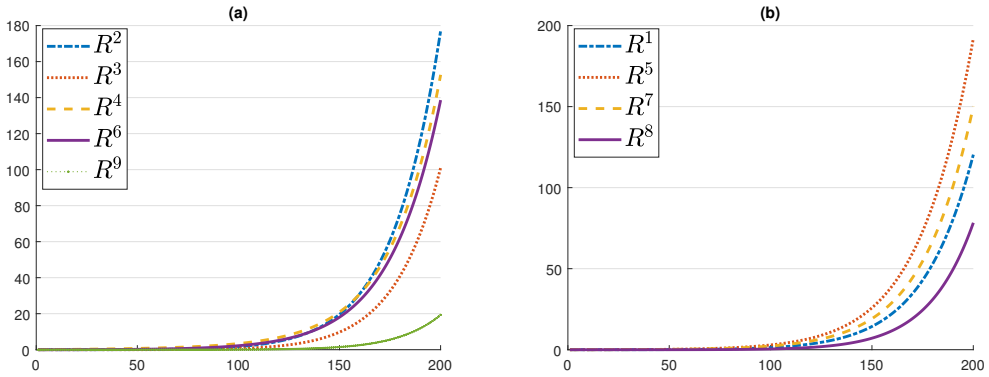

FIGURE 7. Removed without any control

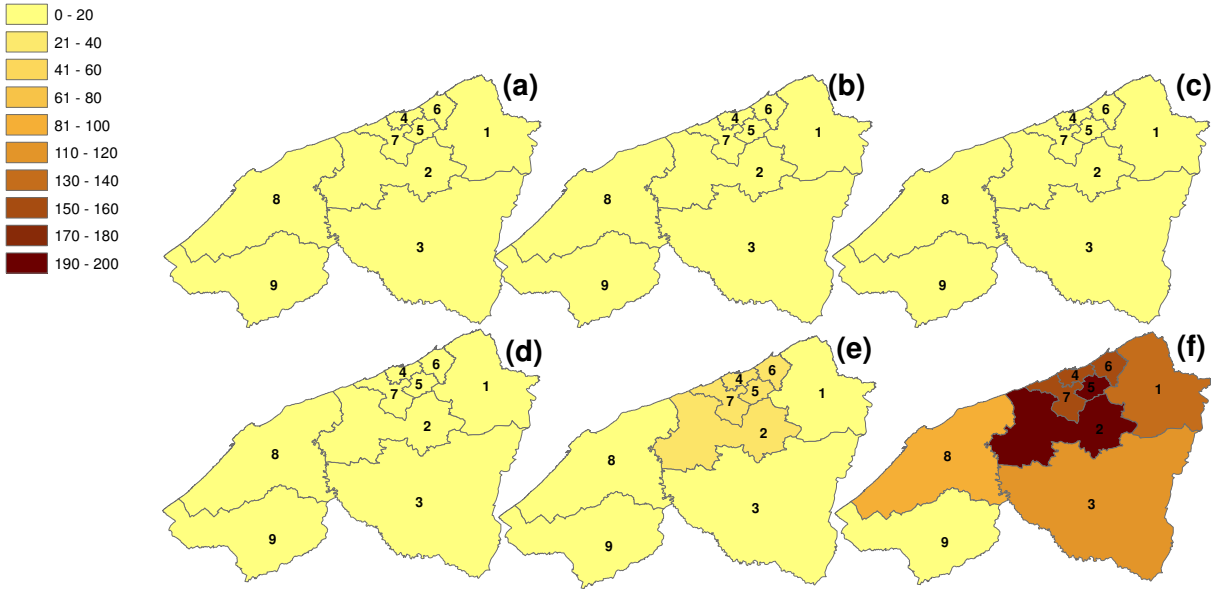

Fig.7 and Fig.6 show the development of the recovered population without controls in the provinces of Casablanca-Settat .

We note that the numbers of the recovered, like the case of the infected, only change from the instant $i = 100$ and gradually increase to reach for the regions C_4 and C_6, C_5, C_7 and C_2 which surrounds the city of Casablanca, small values between 20 and 40 recovered cases .

In the final state $i = 200$ the C_4 region and his neighboring regions were able to reach values between 130 and 200. In the other regions which are geographically further from C_4 have do not exceed the 100 cases at the time $i = 200$.

These simulation show the necessity of some intervention to avoid these huge numbers of infections, especially in the epicenter of the epidemic and the surrounding zones.

FIGURE 8. Susceptibl with the Vaccination control after detecting 200 infections

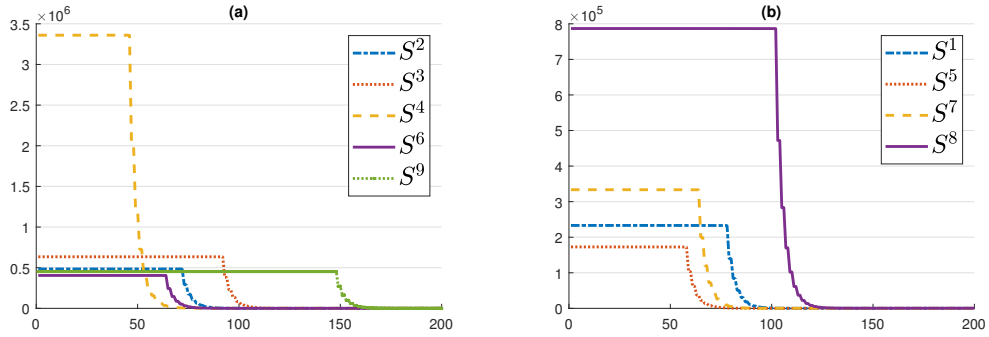

FIGURE 9. Susceptible with the Vaccination control after detecting 200 infections

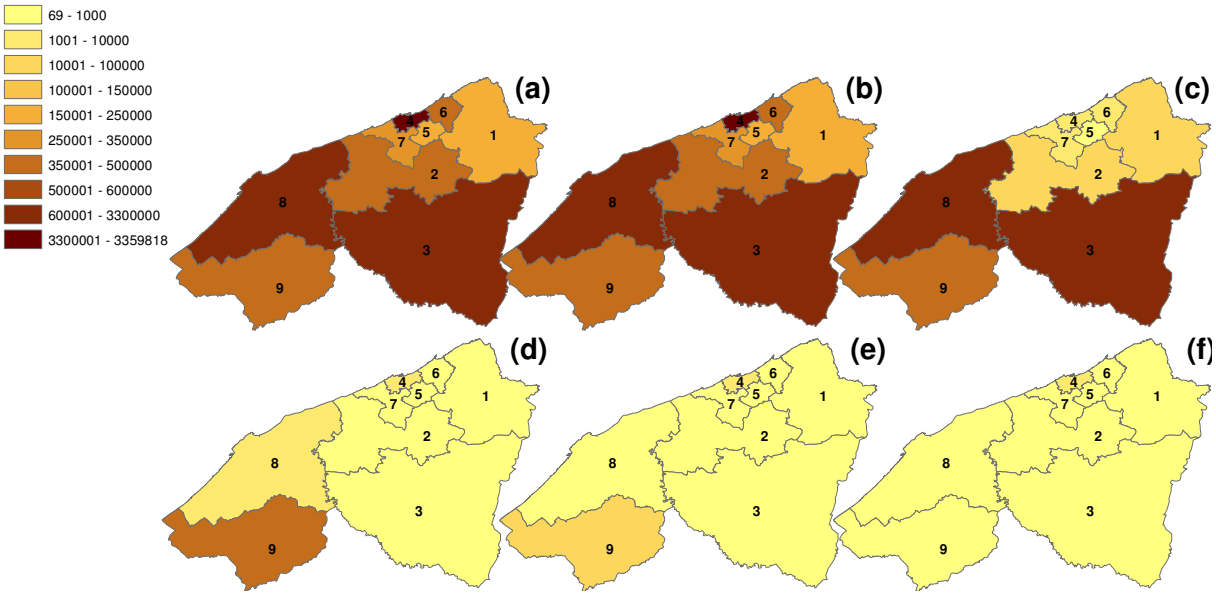

4.4. Scenario 1: Application of the Vaccination control after detecting 200 infections ($I_{min} = 200$). Fig8 and Fig.9 show the evolution of susceptible individuals in the 9 regions by applying the vaccination strategy in a zone after detecting 200 infected people from all regions.

The regions C_1, C_2, C_4,C_5 and C_6 surrounding the Casablanca region decrease rapidly after the moment $i = 50$. The regions which are less distant from C_4 remain constant, then decrease rapidly towards 0.

For regions C_3 and C_8, the susceptible decrease very rapidly towards 0 from the moment $i = 100$. Finally, the regions C_9, which remain constant until $i = 150$, then converge towards 0.

After neglecting the weak presence of susceptible in the different regions, which does not exceed 10^4 in Casablanca C_4, and 10^3 in the other regions (less than 1 of the total population of each region), we can say that after the introduction of a vaccination control after the detection of 200 infected, leads to an almost total disappearance of susceptible from all regions, the evolution of Susceptible in the presence of control from 200 infected (maximum number of regional infected 252 infected) is less important compared to infected in the absence of vaccination control (between 9600 and 76800 infected).

FIGURE 10. infected with the Vaccination control after detecting 200 infections

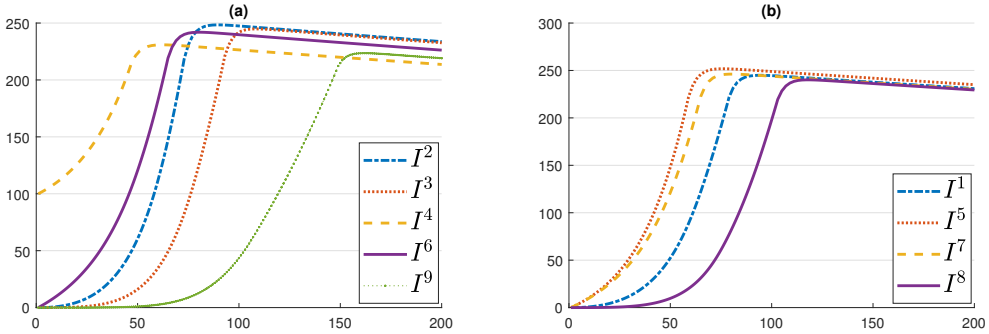

FIGURE 11. Infected with the Vaccination control after detecting 200 infections

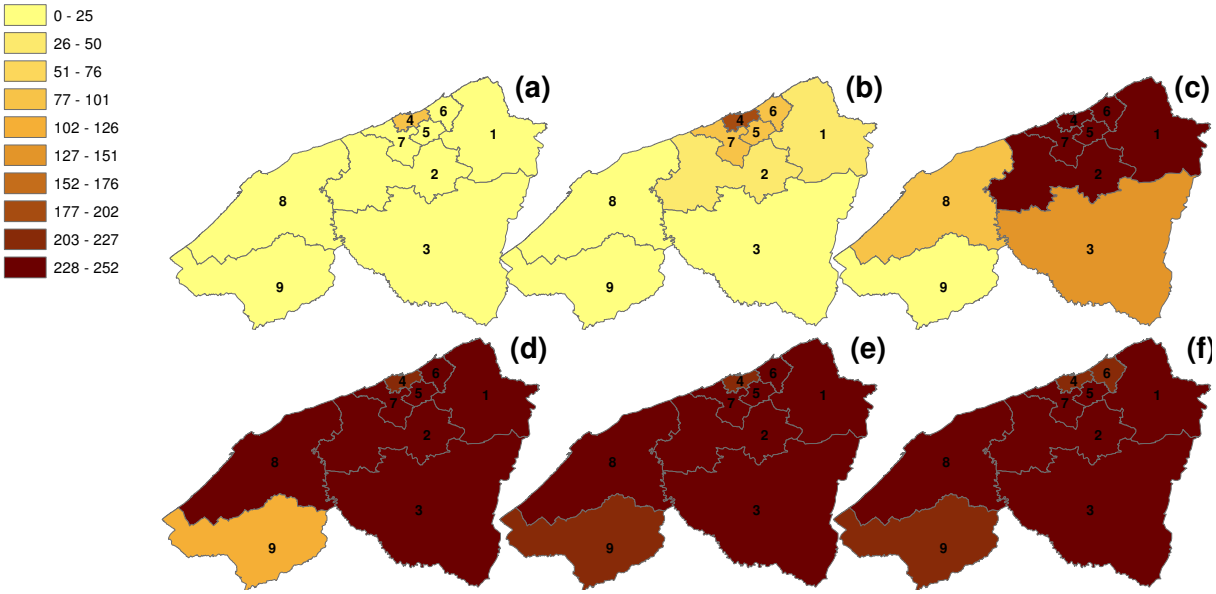

Fig.11 and Fig.10 show the evolution of infected individuals in the 9 regions by applying the vaccination strategy in a zone after detecting 200 infected.

We see in Fig.10 that the number of infected increases up to its maximum value which exceeds 200 infected people from all regions after that it starts to decrease.

The introduction of the control after the ditection of 200 infected, leads to decrease the infection and to keep the number infected always lower than 252 infected. It is quite clear in card Fig.11 that the infection that started from casablanca has spread to the farthest regions.

The evolution of infected in the presence of control from 200 infected (maximum number regional is 252 infected) is less important compared to infected individual in the absence of vaccination control (between 9600 and 76800 infected)

Through the map Fig.11, we note that the disease spreads from the affected region and crawls in the direction of the surrounding regions.

FIGURE 12. romoved with the Vaccination control after detecting 200 infections

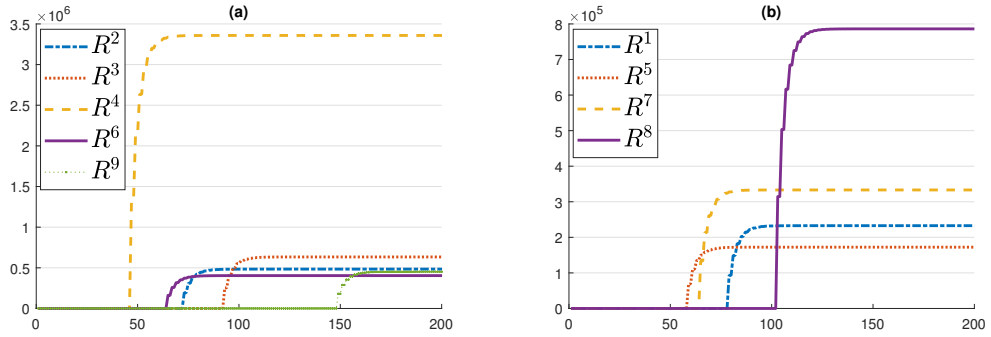

FIGURE 13. Removed with the Vaccination control after detecting 200 infections

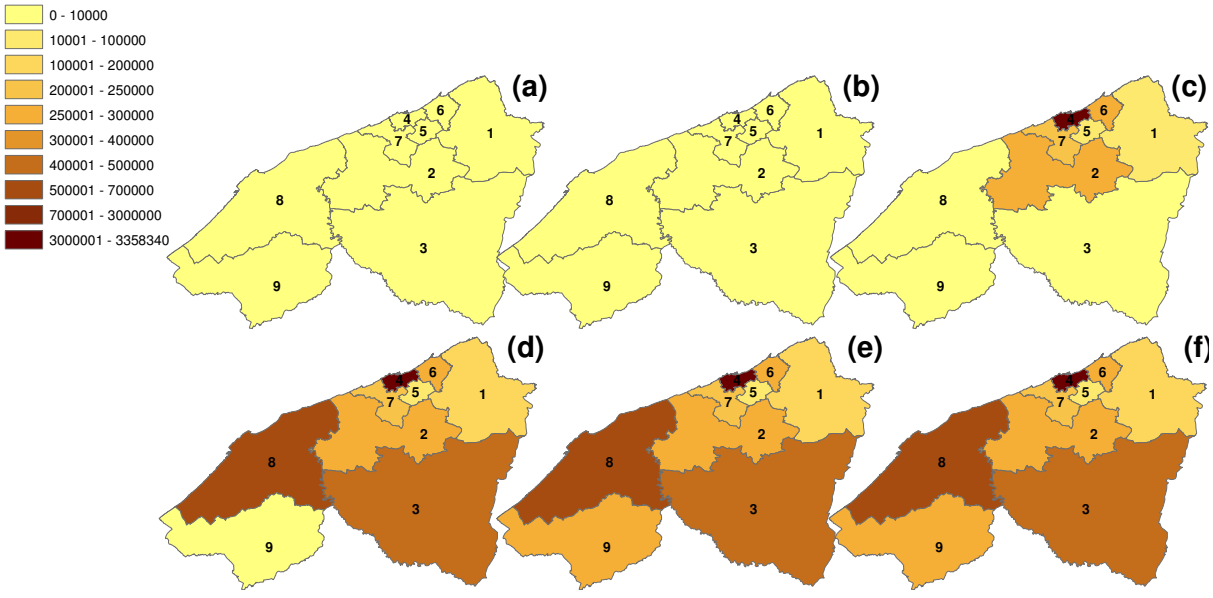

Fig.12 and Fig.13 show the geographical progression and graphs of the cases recovered in the 9 regions by applying the vaccination strategy from 200 infected. We observe that the regions closest to C_4 begin to grow from the moment $i = 120$ reach their maximum values.

We show the geographical progression and graphs of the cases recovered in the 9 regions by applying the vaccination strategy from 200 infected. We observe that the regions closest to C_4 begin to grow from the moment $i = 50$ and reach their maximum values between 1.5 10^5 and 7 10^5 while the region C_4 reaches the maximum of the recovered value about 3.3 10^6, the regions less far from C_4 only grow from the moment $i = 60$ with maximum values between 1.5 10^5 and 5 10^5. On the other hand, the end region begins to grow at the instant $i = 80$. Once the number of infected exceeds 200 cases in a region after reaching a certain time, the number of recovered increases very quickly to reach a maximum value and remains constant after this value which exceeds 1.5 10^5 cases, however without control it does not exceed 200 boxes.

The evolution of Recovered in the presence of control from 200 infected (maximum regional number recovered at the final time $i = 200$ is greater than $10,000$ Recovered) is greater compared to the recovered individual in the absence of vaccination control (maximum regional value of 200 infected), so we can say that the introduction of vaccine control caused a disappearance of susceptible that we can say that they all became Removed if we neglect the small number of infected.

4.5. Scenario 2: Application of the Vaccination control from the beginning of the epidemic ($I_{min} = 0$).

In this scenario we assume that the epidemic is well known in other places, thus, we apply the control interventions from the declaration of such epidemic.

FIGURE 14. Susceptible with the Vaccination control after detecting 0 infections

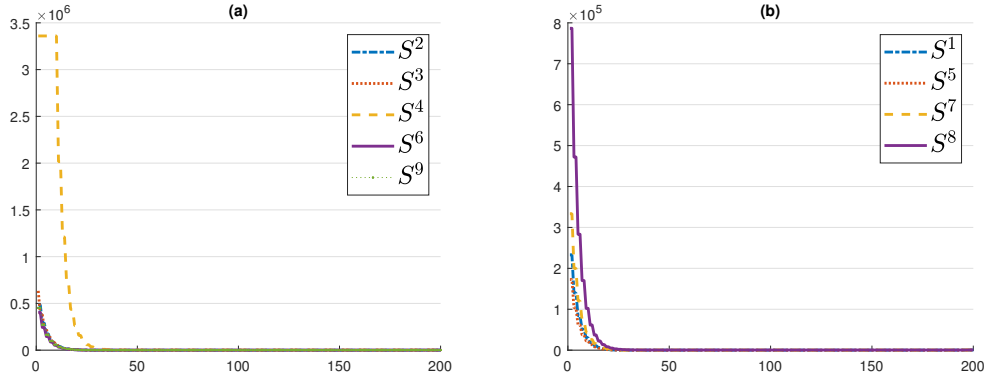

FIGURE 15. susceptible with the Vaccination control after detecting 0 infections

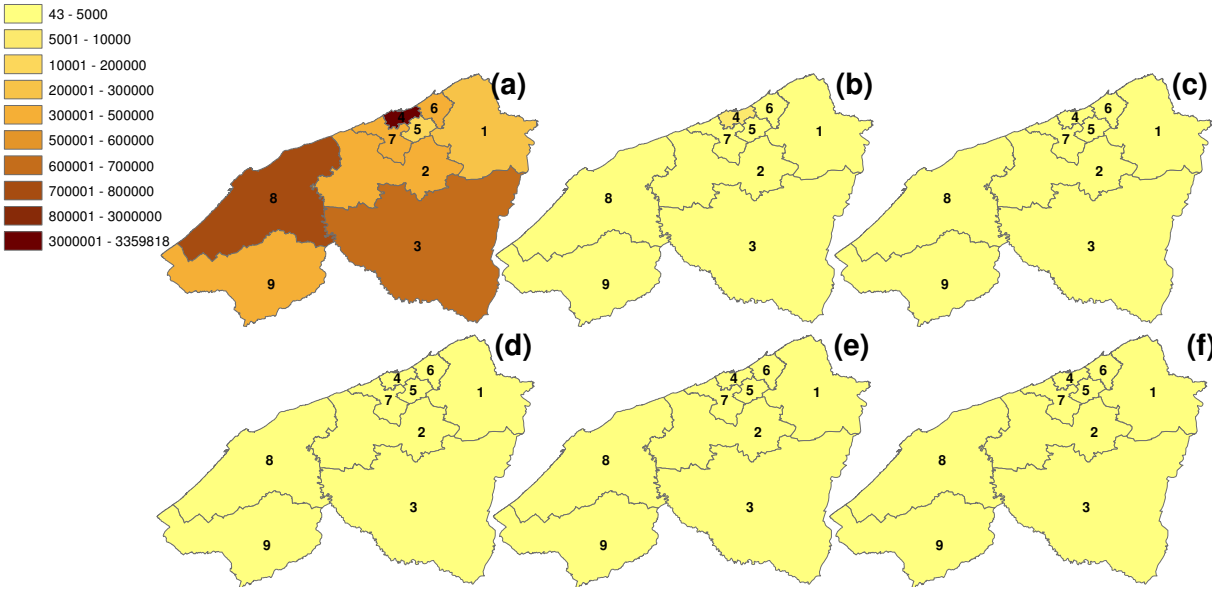

Fig.14 and Fig.15 represent the evolution of susceptible individuals in the 9 regions when applying the vaccination strategy without setting a threshold for infected cases. We note that all the regions except the metropolitan region C_4 know an extreme fall of the susceptible populations, which is canceled very quickly from the instant $i = 25$. For the region C_4 remains at the beginning constant with a value of 3.3 10^6, then decreases from the instant $i = 10$ and is canceled by the instant $i = 25$. Without the threshold for infected people, the susceptible decreases very quickly towards zero, however for the other strategies, the infected must reach the threshold set to begin to decrease.

FIGURE 16. infected with the Vaccination control after detecting 0 infections

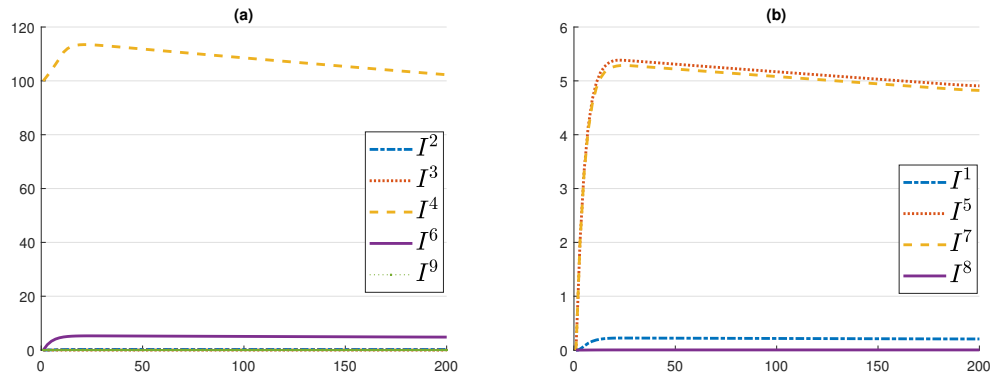

FIGURE 17. Infected with the Vaccination control after detecting 0 infections

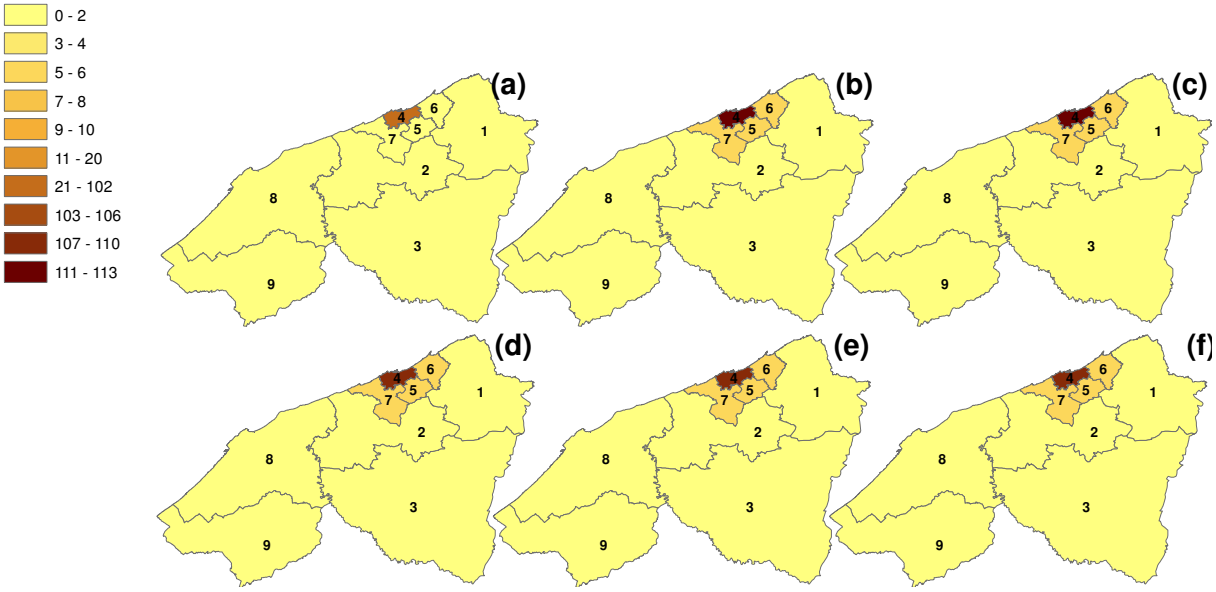

Fig.16 and Fig.17 show the evolution of the infected in the 9 regions by applying the vaccination strategy from the beginning of the epidemic. The number of infections in all regions except regions C_4, C_5, C_6 and C_7 remains almost zero throughout the vaccination period. In the regions C_5, C_6 and C_7 the number of infected increases from 0 without exceeding 6 infected from the moment $i = 10$ decrease until the end of the vaccination. For region C_4 the number of infected rises from 100 cases to 113 at time $i = 20$ and then decreases slightly to reach the value of 100 cases at the end. The infected in the region have a weak growth of 13 cases from times $i = 10$ and decrease until the end. Without the threshold of infected, the number of infected does not exceed 130 cases, but the cost will be very high than of the other scenario.

FIGURE 18. romoved with the Vaccination control after detecting 0 infections

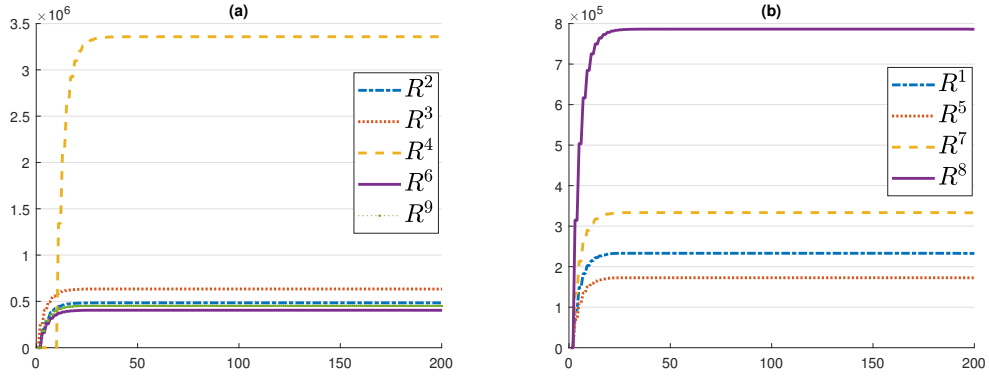

FIGURE 19. Removed with the Vaccination control after detecting 0 infections

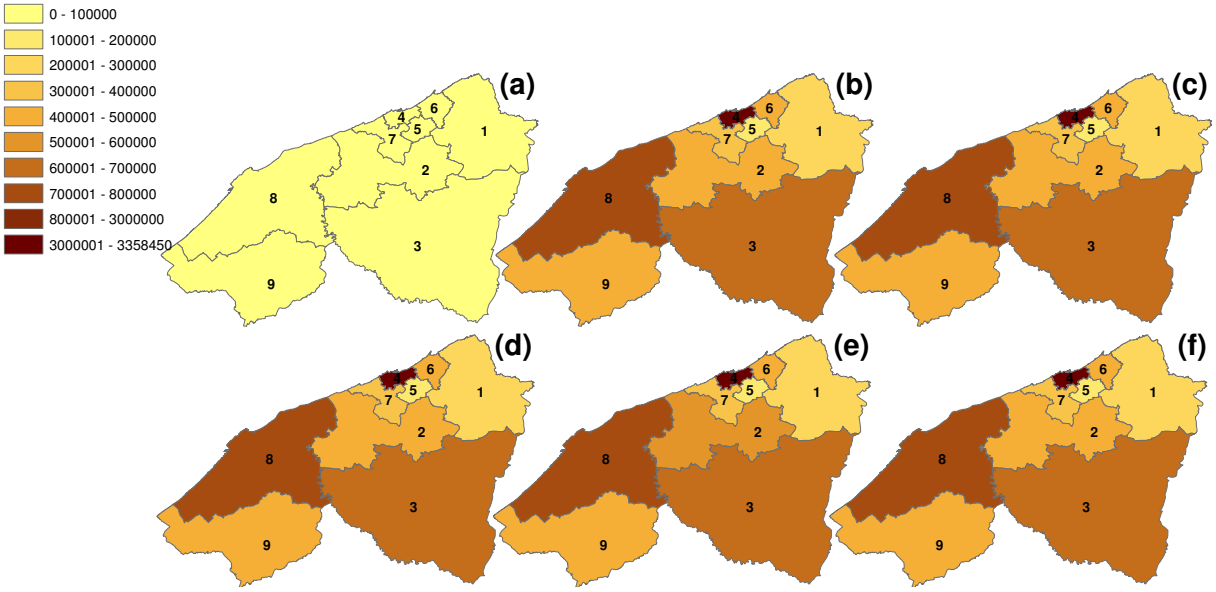

Fig.19 and Fig.18 show the geographical evolution and graphs of the recovered populations in the 9 regions by applying the vaccination strategy without setting any threshold of infection. All regions except the region C_4 recognize a progression of these recoveries from the start to reach maximum values at the instant $i = 15$ and remain constant throughout the period of control. On the other hand, for C_4 it remains almost zero at the beginning until the time $i = 10$ to starts to grow and reaches its maximum value about $3.3\ 10^6$ at the instant $i = 35$, and then remains constant until the end of the period of vaccination. Without the infected threshold, the recovered quickly grows towards its maximum value, however for the other scenario take some time to increase.

5. CONCLUSION

In this paper, we devised a novel optimization approach that represents an extension of the optimal control approach studied in the work of Zakary et al. in the paper [12]. We applied this new approach to a multi region discrete epidemic model SIRS which has been firstly proposed in [10]. We suggested in this article, a new analysis of infection dynamics in M regions which we supposed to be accessible for health authorities. By defining new importance functions to identify affected zones and then will be treated. We investigated the effectiveness of optimal vaccination control approach, we introduced into the model, control

functions associated with appropriate control strategies followed in the targeted regions by mass vaccination campaigns by considering different scenarios. Based on our numerical simulations, we showed the geographical spread of the epidemic and the influence of each region on another and then we deduced the effectiveness of each strategy followed. We concluded that the last scenario of optimal control approach when $I_{min} = 0$ has given better results than the other cases regarding the maximization of the number of removed individuals and minimization of the spread of infection in all regions studied, but this is clearly the most expensive scenario. Thus, as a result, it is necessary to define small thresholds to control the situation as much as possible.

CONFLICT OF INTERESTS

The author(s) declare that there is no conflict of interests.

REFERENCES

[1] Y. Cai, Y. Kang, W. Wang. A stochastic sirs epidemic model with nonlinear incidence rate. Appl. Math. Comput. 305 (2017), 221–240.

[2] J.D. Murray, Mathematical biology, 3rd ed, Springer, New York, 2002.

[3] V. Capasso, Mathematical structures of epidemic systems, Lecture Notes in Biomathematics, 97, Springer-Verlag, New York. 1983.

[4] G.F. Medley, N.A. Lindop, W.J. Edmunds, D.J. Nokes. Hepatitis-b virus endemicity: heterogeneity, catastrophic dynamics and control. Nat. Med. 7 (5) (2001), 619–624.

[5] S.A. Bozzette, R. Boer, V. Bhatnagar, J.L. Brower, E.B. Keeler, S.C. Morton, M.A. Stoto. A model for a smallpox-vaccination policy. New Engl. J. Med. 348 (5) (2003), 416–425.

[6] S.M. Blower, T. Chou. Modeling the emergence of the'hot zones': tuberculosis and the amplification dynamics of drug resistance. Nat. Med. 10 (10) (2004), 1111–1116.

[7] Y.H. Hsieh, Y.S. Cheng. Real-time forecast of multiphase outbreak. Emerg. Infect. Dis. 12 (1) (2006), 122–127.

[8] S. Basu, J.R. Andrews, E.M. Poolman, et al. Prevention of nosocomial transmission of extensively drug-resistant tuberculosis in rural south african district hospitals: an epidemiological modelling study. Lancet. 370 (9597) (2007), 1500–1507.

[9] F. El Kihal, M. Rachik, O. Zakary, I. Elmouki. A multi-regions seirs discrete epidemic model with a travel-blocking vicinity optimal control approach on cells. Int. J. Adv. Appl. Math. Mech. 4 (3) (2017), 60–71.

[10] O. Zakary, M. Rachik, I. Elmouki. On the analysis of a multi-regions discrete sir epidemic model: an optimal control approach. Int. J. Dyn. Control. 5 (3) (2017), 917–930.

[11] O. Zakary, M. Rachik, I. Elmouki. A multi-regional epidemic model for controlling the spread of ebola: awareness, treatment, and travel-blocking optimal control approaches. Math. Meth. Appl. Sci. 40 (4) (2017), 1265–1279.

[12] O. Zakary, M. Rachik, I. Elmouki. A new analysis of infection dynamics: multi-regions discrete epidemic model with an extended optimal control approach. Int. J. Dyn. Control. 5 (4) (2017), 1010–1019.

[13] G. Zaman, Y.H. Kang, I.H. Jung. Stability analysis and optimal vaccination of an sir epidemic model. BioSystems 93 (3) (2008), 240–249.

[14] I. Abouelkheir, M. Rachik, O. Zakary, I. Elmouk. A multi-regions sis discrete influenza pandemic model with a travel-blocking vicinity optimal control approach on cells. Amer. J. Comput. Appl. Math. 7 (2) (2017), 37–45.

[15] B. Hamza, B. Sara, Z. Omar, E. Ilias, F. Hanane, R. Mostafa. SIS multi-regions discrete influenza pandemic model and travel-blocking vicinity optimal control strategy on two forms of patch. Commun. Math. Biol. Neurosci. 2020 (2020), 29.

[16] I. Abouelkheir, F. El Kihal, M. Rachik, O. Zakary, I. Elmouki. A multi-regions sirs discrete epidemic model with a travel-blocking vicinity optimal control approach on cells. Br. J. Math. Comput. Sci. 20 (4) (2017), Article no. BJMCS.31355.

[17] O. Chaturvedi, T. Masupe, S. Masupe. SIRS model for the dynamics of non-typhoidal salmonella epidemics. Int. J. Comput. Eng. Res. 3 (10) (2013), 18-26.

[18] F. Paladini, I. Renna, L. Renna, A Discrete SIRS Model with Kicked Loss of Immunity and Infection Probability, J. Phys.: Conf. Ser. 285 (2011), 012018.

[19] L. Chen, J. Sun. Global stability and optimal control of an sirs epidemic model on heterogeneous networks. Physica A. Stat. Mech. Appl. 410 (2014), 196–204.

[20] O. Zakary, A. Larrache, M. Rachik, I. Elmouki. Effect of awareness programs and travel-blocking operations in the control of hiv/aids outbreaks: a multi-domains sir model. Adv. Differ. Equ. 2016 (2016), 169.

[21] O. Zakary, M. Rachik, I. Elmouki. On the impact of awareness programs in hiv/aids prevention: an sir model with optimal control. Int. J. Comput. Appl. 133 (9) (2016), 1–6.

[22] Masoud Roshanfekr, Mohammad Hadi Farahi, and Raheleh Rahbarian. A different approach of optimal control on an hiv immunology model. Ain Shams Eng. J. 5 (1) (2014), 213–219.

[23] Y. Zhou, Y. Liang, J. Wu. An optimal strategy for hiv multitherapy. J. Comput. Appl. Math. 263 (2014), 326–337.

[24] C. Ding, N. Tao, Y. Zhu, A mathematical model of Zika virus and its optimal control, in: 2016 35th Chinese Control Conference (CCC), IEEE, Chengdu, China, 2016: pp. 2642–2645.

[25] B.N. Kim, K. Nah, C. Chu, S.U. Ryu, Y.H. Kang, Y. Kim. Optimal control strategy of plasmodium vivax malaria transmission in korea. Osong Public Health Res. Perspect. 3 (3) (2012), 128–136.

[26] O. Prosper, N. Ruktanonchai, M. Martcheva. Optimal vaccination and bednet maintenance for the control of malaria in a region with naturally acquired immunity. J. Theor. Biol. 353 (2014), 142–156.

[27] B. Sara, Z. Omar, T. Abdessamad, R. Mostafa, F. Hanane. Parameters' estimation, sensitivity analysis and model uncertainty for an influenza a mathematical model: case of morocco. Commun. Math. Biol. Neurosci. 2020 (2020), 57.

[28] I. Elmouki, S. Saadi. Quadratic and linear controls developing an optimal treatment for the use of bcg immunotherapy in superficial bladder cancer. Opt. Control Appl. Meth. 37 (1) (2016), 176–189.

[29] U. Ledzewicz, H. Schättler. Antiangiogenic therapy in cancer treatment as an optimal control problem. SIAM J. Control Optim. 46 (3) (2007), 1052–1079.

[30] E. Jung, S. Lenhart, Z. Feng. Optimal control of treatments in a two-strain tuberculosis model. Discrete Contin. Dyn. Syst., Ser. B. 2 (4) (2002), 473–482.

[31] D.P. Moualeu, M. Weiser, R. Ehrig, P. Deuflhard. Optimal control for a tuberculosis model with undetected cases in cameroon. Commun. Nonlinear Sci. Numer. Simul. 20 (3) (2015), 986–1003.

[32] G. Hu, J. Geng, Heterogeneity Learning for SIRS model: an Application to the COVID-19, ArXiv:2007.08047 [Physics, q-Bio, Stat]. (2020).

[33] Y. Su, D. Sun. Optimal control of anti-hbv treatment based on combination of traditional chinese medicine and western medicine. Biomed. Signal Proc. Control. 15 (2015), 41–48.

[34] J. Lowden, R.M. Neilan, M. Yahdi. Optimal control of vancomycin-resistant enterococci using preventive care and treatment of infections. Math. Biosci. 249 (2014), 8–17.

[35] S. Bidah, O. Zakary, M. Rachik, H. Ferjouchia. Mathematical modeling of public opinions: Parameter estimation, sensitivity analysis, and model uncertainty using an agree-disagree opinion model. Abstr. Appl. Anal. 2020 (2020). 1837364.

[36] S. Bidah, O. Zakary, M. Rachik. Stability and global sensitivity analysis for an agree-disagree model: Partial rank correlation coefficient and latin hypercube sampling methods. Int. J. Differ. Equ. 2020 (2020), 5051248.

[37] H. Boutayeb, S. Bidah, O. Zakary, M. Rachik. A new simple epidemic discrete-time model describing the dissemination of information with optimal control strategy. Discrete Dyn. Nat. Soc. 2020 (2020), 7465761.

[38] L. Abu-Raddad, F.A. Akala, I. Semini, et al. Characterizing the HIV/AIDS epidemic in the Middle East and North Africa: Time for Strategic Action. Middle East and North Africa HIV/AIDS Epidemiology Synthesis Project. World Bank/UNAIDS/WHO Publication. 2010.

[39] D. Bundy, A. Patrikios, C. Mannathoko, et al. Accelerating the Education Sector Response to HIV: Five Years of Experience from Sub-Saharan Africa. The World Bank, Washington (2010).

[40] K. Dabbs. Optimal control in discrete pest control models. University of Tennessee Honors Thesis Projects, (2010).

[41] L. S. Pontryagin. Mathematical Theory of Optimal Processes, Routledge, London, UK. 2018.

[42] L.S. Pontryagin, V.G. Boltyanskii, R.V. Gamkrelidze. The Mathematical Theory of Optimal Processes. Interscience Publishers, Geneva, Switzerland, 1962.

[43] Nouveau découpage territorial du royaume? *http://www.pncl.gov.ma/fr/News/Alaune/Pages/Nouveau-d%C3%A9coupage-r%C3%A9gional-du-Royaume-.aspx* 2015.

[44] What is a shapefile? *https://desktop.arcgis.com/en/arcmap/latest/manage-data/shapefiles/what-is-a-shapefile.htm* 2020.

[45] what is arcmap? *https://desktop.arcgis.com/fr/arcmap/10.3/main/map/what-is-arcmap-.htm* 2020.

[46] an overview of the neighborhood tools. *https://desktop.arcgis.com/en/arcmap/10.3/tools/spatial-analyst-toolbox/an-overview-of-the-neighborhood-tools.htm* 2020.